Outgrowing neurological diseases: Microcircuits, conduction delay and childhood absence epilepsy

John Milton[1], Jianhong Wu[2], Sue Ann Campbell[3] and Jacques Bélair[4]

[1] W. M. Keck Science Center, The Claremont Colleges, Claremont, CA 91711, USA
jmilton@kecksci.claremont.edu
[2] Laboratory for Industrial and Applied Mathematics (LIAM), Department of Mathematics and Statistics, York University, Toronto, ON, Canada M3J 1P3
wujhhida@gmail.com
[3] Department of Applied Mathematics and Center for Theoretical Neuroscience, University of Waterloo, Waterloo, ON, Canada N2L 3G1
sacampbell@uwaterloo.ca
[4] Département de mathématiques et de statistique and Centre de recherches mathématiques, Université de Montréal, QC, Canada H3C 3J7 and Centre for Applied Mathematics in Biosciences and Medicine, McGill University, Montreal, QC, Canada
belair@dms.umontreal.ca

Summary. The study of familial disorders characterized by recurring changes in neurodynamics, such as epileptic seizures, paralysis and headaches, provide opportunities to identify the mechanisms for dynamic changes in the nervous system. Many of these diseases are channelopathies. The computational challenge is to understand how a constantly present molecular defect in an ion channel can give rise to paroxysmal changes in neurodynamics. The most common of these channelopathies is childhood absence epilepsy (CAE). Here we review the dynamical properties of three neural microcircuits thought to be important in epilepsy: counter inhibition, recurrent inhibition and recurrent excitation. Time delays, τ, are an intrinsic property of these microcircuits since the time for a signal to travel between two neurons depends on the distance between them and the axonal conduction velocity. It is shown that all of these microcircuits can generate multistability provided that τ is large enough. The term "multistability" means that there can be the co-existence of two or more attractors. Attention is drawn to the transient dynamics which can be associated with transitions between attractors, such as delay-induced transient oscillations. In this way we link the paroxysmal nature of seizure recurrences in CAE with time-delayed multistable dynamical systems. The tendency of children with CAE to outgrow their epilepsy is linked to developmental changes in axonal myelination which decrease τ.

Keywords: Childhood absence epilepsy, multistability, time delay, myelination, delay-induced transient oscillations

1 Introduction

Physicians use the evolution of an illness to formulate a diagnosis and guide a treatment plan. Observations as to whether the disease onset is acute or subacute and the course is self-limited, relapsing-remitting or chronic progressive can be sufficient by themselves to significantly reduce the list of possibilities. On the other hand, the experiences of mathematicians and physicists emphasize that careful attention to how variables, namely something that can be measured, change as a function of time, referred to herein as dynamics, can uncover the identity of the underlying mechanisms. From this point of view many diseases may be *dynamical diseases* and arise in physiologial control mechanisms in which critical control parameters have been altered [1, 2, 3]. Consequently important clues related to diagnosis and treatment may be embedded in the time-dependent changes in the relevant clinical variables, such as changes in temperature, weight, blood cells number, the electrical properties of the brain and heart, and so on. As wearable devices for the continuous, non-invasive monitoring of physiological variables become prevalent, it is likely that disease dynamics will increasingly become a focus of attention.

A potentially important application of continuous monitoring of physiological variables arises in the management of a patient with epilepsy. For these patients issues related to patient morbidity, and even mortality, are more often than not due to the unpredictability of seizure occurrence rather than to the seizure itself. For example, seizure occurrence while operating a moving vehicle could potentially be fatal. However, if seizure occurrence could be predicted, then maybe the seizures can be aborted [4, 5, 6, 7, 8, 9]. At the very least it might be possible to give the patient enough time to make arrangements that minimize the effects of the impending seizure.

The study of inherited diseases of the nervous system which are characterized by recurring, paroxysmal changes in neurodynamics would be expected to shed light onto the answers to these questions [10, 11, 12]. In 1995, Milton and Black identified a number of familial disorders characterized by recurring episodes of abnormal neurodynamics (see Table 1 in [13]). Examples of the episodic changes in neurodynamics included epileptic seizures, headaches, paralysis and abnormal movements. They referred to these diseases as *dynamic diseases*. Herein we use the abbreviation DD to refer to both dynamical and dynamic diseases. Many of the DD's identified by Milton and Black were subsequently identified as *channelopathies* (Section 2). Channelopathies arise because of mutations in the genes that encode for the protein subunit components of ion channels of neurons and other exitable cells.

Paroxysmal changes in neurodynamics reflect transient losses in control by neuro-physiological control mechanisms. The goal of this chapter is to identify possible mechanisms for paroxysmal seizure recurrence in childhood absence epilepsy (CAE). CAE is the most common and extensively studied epilepsy associated with a channelopathy (Table 1). There are two important issues: 1) How can a constantly present molecular defect give rise to the recurring

seizures exhibited by the patient ? (Sections 5-7) and 2) Why do seizures in CAE appear during childhood and then typically abate by late adolescence ? (Section 8). Our literature review links the paroxysmal nature of seizure occurrence to dynamical systems which contain time delays and which exhibit multistability. The tendency of children with CAE to outgrow their seizures is linked with changes in τ related to developmental changes in brain myelination. Finally we discuss our findings in Section 9.

2 Dynamic diseases in neurology and psychiatry

A practical problem for identifying the critical parameters and underlying control mechanisms for DD is that it is not often possible to monitor the patient at the time the dynamics change. For this reason patients in which paroxysmal events recur with a certain predictability are ideal candidates to characterize the nature of the DD transition. Thus it becomes possible, at least in principle, to use techniques such as multimodal imaging to document the structure of the brain and the physiological changes that occur at the time the changes in dynamics occur. The hope is that as more and more events are recorded, it may be possible to identify the common features and hence the critical control parameter(s).

Tables 1 and 2 summarize two groups of DD's of the nervous system that are potentially well suited for determination of how paroxysmal changes in signs occur [12]. The first group includes those diseases in which paroxysmal events can be repeatedly triggered with a certain predictability. The second group includes those neurological and psychiatric disorders that appear in infancy-childhood and then spontaneously disappear as the child gets older, typically by mid to late adolescence (Table 2). It should be noted that the clinical use of the words "periodic" and "paroxysmal" differs from their mathematical meaning. Typically physicians use the term "periodic" to mean that the signs recur "every so often" or "every once in a while". The term "paroxysmal" means that the onset of the signs occurs suddenly and without warning.

An exciting development has been the realization that many of the familial paroxysmal and periodic neurological diseases are channelopathies. Ion channels are the transmembrane pores which allow ions to flow across membranes in response to their electrochemical gradients. Although ion channels can be formed by a single protein (e.g., the transmembrane chloride conductance regulator in cystic fibrosis [14]), most often ion channels are formed from an assembly of protein subunits each encoded by a different gene. Over 400 ion channel genes have been identified: a useful resource is the Online Mendelian Inheritance in Man (OMIM) website: `www.ncbi.nlm.nih.gov/omim`.

Many of the DD's in Tables 1 and 2 are associated with gene mutations related to various ion channels including the voltage-gated Ca^{++}, Cl^{-}, K^{+}, and Na^{+} channels and the ligand-gated acetylcholine nictonic and γ-aminobutyric acid A ($GABA_A$) receptors. These ion channels are the "excitable" in the

Table 1. Gene mutations in neurological DD's characterized by paroxysmal events

Dynamic disease[a]	Mutated gene[b]	Triggering events[c]
Channelopathies		
Andersen-Tawil syndrome	Kir2.1	None
Benign familial neonatal epilepsy	SCN2A	?
Childhood absence epilepsy	GABRA1, GABRA6, GABRB3, GABRG2, CACNA1H	hyperventilation
Familial hemiplegic migraine	CACNA1A	minor head trauma, cerebral angiography
Familial hyperplexia	GRAR1, GLRB	unexpected auditory or tactile stimuli
Familial paroxysmal ataxia	CACNA1A, KCNA1,CACNB4	stress, excitement
Hyperkalemic periodic paralysis	SCN4A	fasting, exercise, K^+ foods
Hypokalemic periodic paralysis	CACNA1S, SCN4A	insulin, glucose
Juvenile myoclonic epilepsy	DRD2, CACNB4, CLCN2 GABRA1, GABRD, EFHC1	awakening
Nocturnal frontal lobe epilepsy	CHRNA4, CHRNB2, CHRNA2	Sleep I-II transition
Paroxysmal choreoathetosis/spasticity	SLC2A1	alcohol, exercise, sleep deprivation, stress
Paroxysmal non-kinesigenic dyskinesia	MR-1	alcohol, coffee, stress, fatigue
Paroxysmal kinesigenic dyskinesia	PRRT2	sudden voluntary movement

[a] Clinical descriptions of these disorders and the identification of the gene mutations associated with these disorders can be found on the OMIM website (see text).
[b] Site of mutation: voltage-gated calcium channel (CACNA1A, CACNA1H, CACNA1S, CACNB4), cloride channel (CLCN2), dopamine receptor (DRD2), inward-rectifying potassium channel (Kir2.1), voltage-gated potassium channel (KCNA1), voltage-gated sodium channel (SCN4A), acetylcholine nictonic receptor (CHRNA4, CHRNA2, CHRNB2), glycine receptor (GLRA1, GLRB), $GABA_A$ receptor (GABRA1, GABRA6, GABRB2, GABRB3), acetylcholine nictonic receptor (CHRNA4, CHRNA2, CHRNB2), proline rich transmembrane protein (PRRT2), major histocompatibility complex related gene protein (MR-1), solute carrier gene (SLC2A1).
[c] The triggering events refer to stimuli and behaviors most often reported by patients as precipitants of "their attacks".

term excitable cell. The work of Hodgkin and Huxley links the dynamics of excitable cells to the properties of the ion channels located in their membranes. These models take the general form

$$C\dot{V}(t) = -I_{\text{ion}}(V, W_1, W_2, \cdots, W_n) + I_0 \tag{1}$$
$$\dot{W}_i(t) = \beta \frac{[\hat{W}_i(V) - W_i]}{\Gamma(V)}$$

where $V(t)$ is the membrane potential, Γ is a time constant, C is the membrane capacitance, I_{ion} is the sum of V-dependent currents through the various ionic channel types, I_0 is the applied current, W_i describe the fractions of channels of a given type that are in various conducting states (e.g., open versus closed), $\hat{W}_i(V)$ describe the equilibrium functions and β is a temperature-like time scale factor.

Over 50 years of work by mathematicians and neuroscientists have established a quantitative agreement between experimental observations on neurons and the predictions of (1) (for review see [15, 16, 17, 18, 19, 20]). The predicted neuronal spiking dynamics include a variety of regular spiking and bursting patterns. It can be anticipated that it should be possible to draw analogies between abnormal neurodynamics and the clinical presentations. However, neurons are not the only type of excitable cell. Cardiac and skeletal muscles and certain endocrine cells such as pancreatic β-cells are also excitable. Thus it is not difficult to appreciate the complexity of the clinical presentations and inheritance patterns of this group of diseases [21, 22].

3 Childhood absence epilepsy (CAE)

CAE is a channelopathy that exhibits both paroxysmal dynamics and a developmental pattern (Tables 1 and 2). Many families with absence epilepsy have a defect in one of the subunits of the γ-aminobutyric acid A (GABA_A) receptor. The GABA_A receptor is an anion selective, ligand-gated ion channel [23]. The concept that CAE reflects a disturbance of inhibition is supported by both animal and human observations. For example, in cats, systemic injection of penicillin, a weak GABA_A receptor antagonist, causes a dose-dependent transformation of sleep spindles to spike-wave discharges (SWD), the electroencephalographic (EEG) signature of CAE [24, 25]. In human CAE, GABA-mimetic anti-epileptic drugs such as vigabatrin and tiagabine exacerbate absence seizures [26, 27].

Seizure onset is between the ages of 4-6 years and most commonly the seizures disappear by mid to late adolescence. There are no long term cognitive or behavioral sequelae. The seizures occur abruptly without warning and consist of brief spells of staring and unresponsiveness typically lasting 10-20s. Minimal myoclonic jerks of the eyes and perioral automatisms can often be observed during the seizure. The frequency of the spells can be very high (100's per day). The EEG recorded using electrodes placed on the scalp changes during the seizure demonstrate the presence of generalized 3-4 Hz SWDs (Figure 1a). Typically the seizure can be triggered at the bedside by

Table 2. Paroxysmal neurological dynamic diseases of childhood and adolescence which may be outgrown.

Dynamic disease[a]	Mutated gene[b]	Triggering events	Outgrown by[c]
Epilepsy			
Benign familial infantile epilepsy	PRRT2		18 months
Benign familial neonatal epilepsy	SCN2A		7 yrs
Benign rolandic epilepsy	11p13	awakening	adolescence
Absence epilepsy	GABRA1, GABRA6, GABRB3, GABRG2, CACNA1H	hyperventilation	adolescence
Juvenile absence epilepsy	EFHC1	awakening	3^{rd}-4^{th} decade
Juvenile myoclonic epilepsy	DRD2,CACNB4, CLCN2, GABRA1, GABRD, EFHC1	awakening	3^{rd}-4^{th} decade
Occipital epilepsy	?	?	adolescence
Familial hyperekplexia	GLRA1, GLRB	unexpected auditory or tactile stimuli	childhood
Motor tics			
Tourette's syndrome	?	anxiety, stress	adolescence
Parasomnias			
Bed wetting	?		adolescence
Night terrors	?		adolescence
Sleep walking	20q12-q13.12	stress, alcohol, sleep deprivation	adolescence
Sleep talking	?		adolescence
Speech disorders			
Stuttering	?		adolescence

[a] Clinical descriptions of these disorders and the identification of the gene mutations associated with these disorders can be found on the OMIM website.
[b] Site of mutation: EF-hand domain containing protein 1 (EFHC1), gene mutation located on short arm of chromosome 11 (11p13), gene mutation long arm of chromosome 20 (20q12-q13.12). See also legend for Table 1.
[c] These estimates are the most commonly observed age at which the troubling clinical signs disappear.

having the child hyperventilate. Seizures in CAE can often be aborted using brief sensory stimuli, for example, the mother shaking or speaking to the child, a loud noise. The ability of sensory stimuli to abort seizures can also be observed in patients with atypical absence seizures characterized by 1.5-2.5 Hz SWDs (Figure 1b) [28].

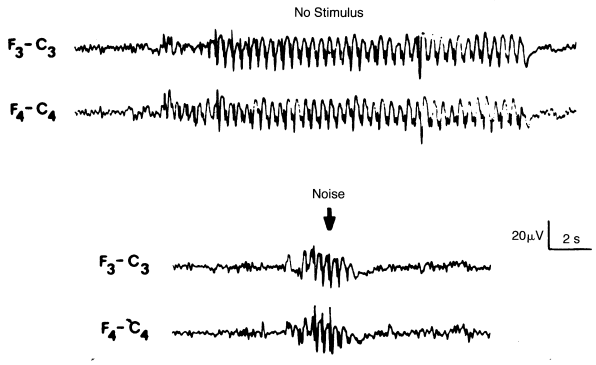

Fig. 1. Top: Scalp EEG changes recorded during a generalized seizure in 16 year old with atypical absence epilepsy. Bottom: The application of a brief sensory stimulus can shorten the length of the seizure. Figure reproduced from [28] with permission.

Current debates concern the mode of onset of absence seizures in CAE [29, 30]. At the bedside, the classification of epileptic seizures was based on how a seizure begins in the first split second as determined by 1) direct observations of the clinical aspects of the seizure, and 2) correlation between the clinical features of the seizures and the changes detected in the EEG. If the seizure began in a focal area of the brain it was called a *partial epileptic seizure*. If the seizure appeared to begin everywhere at the same time it was called a *primary generalized seizure*. Thus historically seizures in CAE were considered to be primary generalized.

However, the use of scalp EEG recordings is not sufficient to rule out the possibility that absence seizures in CAE have a focal onset. For example, it would be very difficult to distinguish a generalized seizure from a focal onset seizure which rapidly generalizes. Indeed simple calculations based on estimates of seizure propagation velocities suggest that the fastest way to generalize a seizure is via reciprocal cortico-thalamic connections [31]. Depth electrode recordings in patients with generalized seizures were the first to demonstrate that seizure foci located in the frontal lobes could so rapidly generalize that a focal onset would be missed from scalp EEG recording [32, 33].

A cortical site for absence seizure onset has been identified in a rodent model for absence seizures [34]. It is located in peri-oral somatosensory cortex. Recently high resolution EEG-MEG studies together with advanced signal

analysis techniques of absence seizures in human CAE have shown the presence of localized areas of pre-seizure activation in frontal cortex, orbito-frontal cortex, the mesial temporal lobe and the parietal lobe [35, 36, 37]. These observations are reminiscent of the concept developed for partial complex seizures that emphasizes the role of a spatially extended *epileptic system* that regulates the onset, maintenance and cessation of partial epileptic seizures [38, 39].

The above observations indicate that seizures in CAE are *secondarily generalized*. Here we focus our attention on the dynamics of seizure onset and do not consider how the epileptic activity spreads from the epileptic focus once the seizure is initiated.

4 Dynamical systems approaches to seizure onset

At the most basic level, a seizure represents a change in the activity of neurons. The cortical interictal state is primarily characterized by low frequency neuronal spiking [40, 41]. The hallmark of the onset of a seizure is a change in neural spiking rates.

Dynamics is concerned with the description of how variables, such as those related to neural spiking rates, change as a function of time. The fact that the magnitude of a variable in future time will be known once we know its initial value and rate of change per unit time is a fundamental property of the differential equation

$$\dot{x} \equiv \frac{dx}{dt} = f(x)\,, \tag{2}$$

where x is, for example, the firing rate. The left-hand side of this equation re-iterates the importance of the change in the variable per unit time and the right-hand side states the hypothesis proposed to explain the time-dependent changes in the variable. In this chapter we are particularly interested in the role played by factors related to the physical separation of neurons on seizure onset. These factors include the axonal conduction velocity, v, and the distance, r, between neurons. Consequently (2) becomes the delay differential equation (DDE)

$$\dot{x} = f(x(t-\tau))\,, \tag{3}$$

where $\tau = r/v$ is the time delay. An introduction to the numerical methods available for the analysis of (3) is given in Appendix A. In order to obtain a solution to (3) it is necessary to specify an initial function, ϕ, on the interval $[-\tau, 0]$. These initial values can be changed using brief external stimuli. This observation is relevant to the clinical observation that brief sensory and electrical stimuli can abort an absence seizure. From a dynamical systems point of view this observation suggests *multistability*. To understand what is meant by the term multistability, we need to consider the nature of the solutions of (3).

Solutions of (3) can be classified by the qualitative nature of the changes in the variable as a function of time. Fixed point solutions are solutions where the

values of the variables are fixed in time. Such solutions would correspond to a constant neural spiking rate. Periodic solutions are solutions which oscillate in time with some fixed period. Such solutions would correspond to oscillatory changes in spiking rate such as seen for a bursting neuron or population.

Another way that solutions can be classified is with respect to their response to perturbations. From this perspective a solution is called *stable* if solutions which have initial conditions close to the solution approach it in the longterm, otherwise it is called *unstable*. Stable solutions will be observed in numerical simulations and experiments. Unstable solutions will not persist in the longterm, but may be observed transiently. It is possible that an unstable solution may correspond to a seizure [12]. *Multistability* refers to the situation when there is more than one stable solution in the system: the long term behavior of the system then depends on the starting, or initial conditions and whether they system is subjected to any perturbations. If a system has multiple stable solutions, then it must also have unstable solutions.

A *parameter* is a variable which changes so slowly in comparison to the time scale of the variables of interest that it can be regarded as constant. Examples of parameters relevant for the occurrence of an absence seizure include τ, the number of GABA receptors, the receptor binding constant for GABA, the parameters that govern the gating of the Cl^- channel, and so on. We will be particularly interested in how the number, type and stability of solutions change as one or more parameters are changed. This is called a *bifurcation*. Parameter values where this occurs are called *bifurcation points*. When a bifurcation occurs in a system, the qualitative behaviour of the system changes. For example, the system may transition from having a stable fixed point as the long-term behavior to having a periodic solution as the long-term behavior.

In summary, we use DDEs to describe the neurophysiological rules that govern the change rates of the system variables. These equations are often nonlinear and often involve neural physiological properties such as decay rates of action potentials and gains, and interconnectivity of the population such as synaptic connection weights, conduction velocities and time delays. These neurophysical properties, synaptic weights and conduction velocities remain constant in the time scale of the considered neurodynamics, and are called parameters. Naturally, solutions of the DDEs depend on both their initial values and the parameters. Understanding dynamic diseases in systems described by a DDE requires the examination of behaviors of solutions - evolutions with respect to time of the variables - for a wide range of plausible initial conditions and parameter values of the system. An important property of a dynamical system is the emerging long-term behaviors, in which solutions from a set of different initial conditions may converge to a particular solution which is called an attractor. The set of initial conditions for which the corresponding solutions converge to the attractor is called the basin of attraction. A dynamical system may have multiple attractors for a particular parameter value. This is called multistability. The same system with two different parameters

may have different numbers and types of attractors, the critical values of parameters through which the system undergoes changes (bifurcations) in the numbers and types of attractors are called bifurcation points. Often these attractors take the form of fixed point solutions or limit cycles or periodic solutions.

In Section 7.2 we outline how to determine the number and stability of fixed points of a model, the nature of the possible bifurcations as a function of τ and the conditions for the occurrence of multistability. Our particular focus is on the situation when the time delay acts a bifurcation parameter. In order to improve the flow of the presentation of the mathematical results, we will not give references for all the standard results we use: these can be found in [42, 43, 44], and a more complete (and abstract) approach to the theory of delay differential equations can be found in [45] or [46].

5 Paroxysmal seizure occurrence

The hallmark of epilepsy is the paroxysmal nature of seizure occurrence [28, 47] which can even be observed in human neocortical slices [48]. Many computational models of absence seizures have examined topics related to the identification of the mechanism of action of anticonvulsant medications, the generation of the EEG and the nature of the mechanisms that recruit large populations of neurons into the evolving seizure (for reviews see [49, 50, 51, 52, 53]). Much less attention has been given to understanding how a seizure begins when it does and why a seizure, once started, eventually stops (for notable exceptions see [28, 47, 54]).

We take a dynamical systems approach. Our concern is on the dependence of the solutions of the governing differential equations as regulating parameters (e.g., nerve fiber length, conduction velocity) are changed and where these solutions start from. Qualitative changes in these behaviors are called *bifurcations*. To be more specific, we briefly recall here some basic concepts relevant to dynamical systems in the context of DDEs. Under this paradigm, there are four general types of mechanisms in delay differential equations that can produce a paroxysmal change in dynamics (Figure 2). Two of these mechanisms involve changes in parameters and two involve changes in variables.

The first mechanism proposes that sudden changes in dynamics arise because of a change in an important parameter such as a feedback gain or τ [1, 2, 3, 55]. The changes in dynamics correspond mathematically to bifurcations in the relevant nonlinear equations which describe the affected physiological system. Examples of DD's which can be attributed to this mechanism include Cheyne-Stokes respiration [2] and blood cell diseases characterized by oscillations in blood cell number [56, 57, 58]. In terms of an explanation for an absence seizure this approach requires two parameter changes: one parameter change to explain the seizure onset, another to explain why the seizure stops.

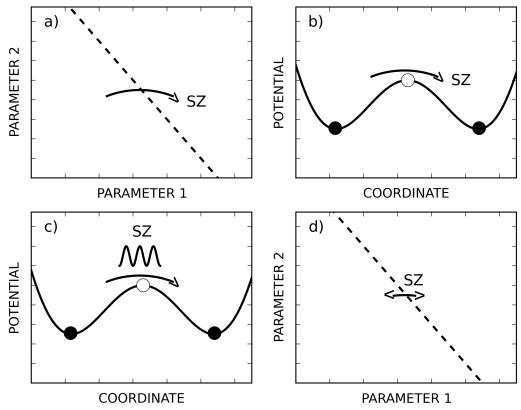

Fig. 2. Four mechanisms for producing a seizure (SZ). (a), a bifurcation caused by moving a parameter across a stability boundary (dashed line), (b) a change between two attractors caused by changes in the initial conditions, (c) a transient unstable oscillation which arises as the system moves from one attractor to another, (d) critical phenomena that arise when the dynamical system is tuned very close to a stability boundary (dashed line).

The idea that seizure onset in CAE is related to changes in variables is based on clinical observations (Figure 2b). A brief sensory or electrical stimuli corresponds to a change in the initial function ϕ. This observation is suggestive of a multistable dynamical system [28, 47]. Figure 2b illustrates this concept of a dynamical system using the potential energy surface, $U(x)$. The minima ("valley") corresponds to a stable solution and the maxima ("hill") represent an unstable solution. In this interpretation, the onset of a seizure corresponds to a transition from one valley to the next, or in other words, a transition into a basin of attraction associated with a seizure. Brief stimuli abort the seizure by causing a transition from the seizure-related basin of attraction to one associated with healthy brain dynamics. This mechanism for an absence seizure also requires two changes in the variables: one change to explain seizure onset, another to explain why the seizure stops.

There are two mechanisms which incorporate both the onset and cessation of the seizure. The first involves modification of the multistability concept (Figure 2c). It relies on the observation that in time-delayed dynamical systems, an unstable limit cycle can be associated with the separatrix that separates two stable attractors [12, 59, 60, 61], i.e. the "hump" between the "two valleys". It must be emphasized that the stable attractors do not correspond to the seizure, the seizure arises as a transient oscillation associated with the transition between the attractors [10, 12]. In the two-neuron micro-

circuits discussed in Section 7.2 delay-induced transient oscillations (DITOs) are associated with the presence of an unstable limit cycle [59, 60].

The final mechanism is based on the concept that the parameters of neural control mechanisms are tuned very close to the "edge of stability" (Figure 2d). Indeed excitatory synaptic inputs to pyramidal neurons outnumber the inhibitory ones by 6.5 to 1 [62]. The fundamental concept is that a seizure might correspond to a phase transition. Thus near the bifurcation point, a dynamical system is expected to be characterized by collective behaviors for which it is not possible to define a specific correlation length. There are two clinical observations consistent with this hypothesis. First, the distribution of seizure sizes and times to occurrence exhibit power law behaviors [6, 63, 64, 65]. Second, even for individuals who do not have clinically-evident seizures, micro-seizures can be observed while the subject sleeps [66]. Thus from this point of view clinical epilepsy is a disease which is characterized by larger events [67]. However, dynamical systems tuned toward the edge of stability are also expected to generate a number of critical phenomena, such as critical slowing down and amplitude amplification [68]. These phenomena have not been observed for the majority of seizure occurrences [69].

6 Epileptic micro-circuits

Simultaneous recording of thalamic and cortical local field potentials during an absence seizure in CAE demonstrated that the oscillations are detected in the thalamus 1-2s before SWDs are observed in the cortex [70]. Thus it is currently believed that the SWDs recorded by the scalp EEG during absence seizures are generated by the thalamo-cortical-thalamo circuit shown in Figure 3 [71]. This network involves reticular thalamic neurons (nRT), thalamic relay neurons (TC) and cortical pyramidal neurons (CT). Inhibitory connections occur in both the thalamus and the cortex. This same circuit is involved in sleep and early investigators quickly recognized that the very mechanisms that generate sleep spindles are "hijacked" in CAE to generate the SWD [24, 25, 72].

It is useful to keep in mind that the thalamocortical circuit shown in Figure 3 is for a rodent model of absence epilepsy [73]. However, much of the early work on absence seizure was done on feline brains [24, 25]. There are important physiological and anatomical differences between the thalamus of rodents and felines. For example, in rodents inhibitory interneurons are absent in almost all thalamic relay nuclei [74]. Thus intrinsic inhibition is absent in most of the thalamus and inhibition relies almost entirely on input from nRT. In contrast, in the feline thalamus, intrinsic GABAergic inhibitory interneurons are present throughout the thalamus, including its relay nuclei. Here the nRT provides an additional external inhibitory input. The thalamus in humans is much more developed that in rodents and felines [74, 75] and hence we can expect even more differences.

For unmyelinated axons, $v \sim \sqrt{d}$, and for myelinated axons, $v \sim dg\sqrt{\ln g}$, where d is the axon diameter and g is the ratio of d to overall fiber diameter. From Figure 3 it can be seen that there is a distribution in the length of interneuronal axons: the length of axons associated with the intrathalamic connections (nRT $\leftrightarrow$ TC) are shorter ($<$ mm's) than those associated with thalamo-cortical connections (CT $\leftrightarrow$ nRT and CT $\leftrightarrow$ TC) ($\sim$ cm's). Since $\tau = r/v$, we can anticipate that there will be a bimodal distribution of τ [76]. This segregation in terms of short and long τ is further increased by the facts that 1) many of the cortico-thalamic axons are unmyelinated [77] (hence τ is increased) and 2) gap junctions exist between nRT neurons [78, 79] (hence τ is decreased).

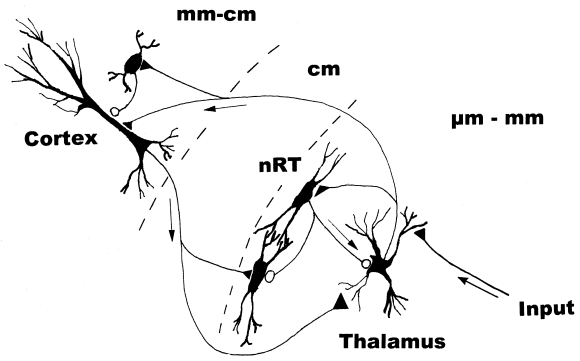

Fig. 3. Corticothalamic circuit involved in the genesis of absence seizures and sleep spindles. The cortical-thalamic distances between neurons are of the order of $\sim$ 5cm and those within the thalamus are $<$ 1mm. The cortico-cortical distances range from $<$ 1mm to $5 - 10$cm.

It is increasingly being recognized that the behavior of large ensembles of neurons can be understood from smaller motifs involving 2-3 neurons [80, 81, 82]. Figure 4a shows four microcircuit motifs which have been emphasized for the generation of epileptic seizures [81]: 1). recurrent inhibition (RI), 2) counter inhibition (CI), 3) recurrent excitation (RE) and 4) feedforward inhibition (FFI). For CAE, the $GABA_A$ defect draws attention to those microcircuits which include an inhibitory component. Thus the thalamo-cortical ciruit shown in Figure 3 can be interpreted as a FFI microcircuit (Figure 4 a and b). Indeed the FFI microcircuit has been considered to be critically important for the generation of SWD recorded by the EEG.

However, recent observations cast doubt on the importance of the FFI microcircuit for seizure onset [73]. First, seizures occur in the $Gria4^{-/-}$ mice in which the connection between nRT and CT neurons has been deconstructed with optogenetic techniques [83]. Second, studies of olfactory cortex suggest that whereas FFI and excitation are balanced, RI dominates the intracorti-

cal excitations which are highlighted in our analysis [84]. Finally, as already pointed out, absence seizures in CAE have a focal cortical onset. From a mathematical perspective, FFI requires a model that involves three neurons. Investigations of similar models [85] have shown that that the delay effects we outline below likely do not play a role in such a circuit when it is isolated. More complex nonlinear effects involving interactions with other microcircuits [86] may be required to generate the multistable dynamics we emphasize here. Therefore in the discussion which follows we emphasize the role of RI, RE and CI for seizure onset.

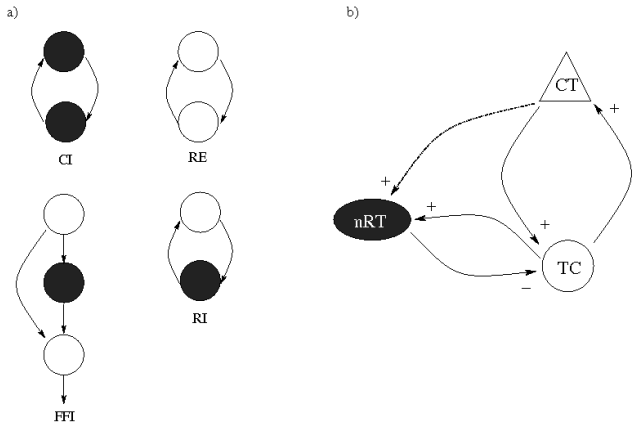

Fig. 4. Four neural micro-circuits important for the generation of epileptic seizures. (a) recurrent inhibition (RI), counter inhibition (CI), recurrent excitation (RE) and d) feedforward inhibition (FFI). (b) Thalamocortical circuit important for CAE. The dark neurons are inhibitory and the white faced ones are excitatory.

7 Multistability in time delayed microcircuits

The dominant theme of our discussion is that DDE models for the CI, RI and RE microcircuits readily generate multistable dynamics. This multistability is defined as the simultaneous co-existence, for fixed parameter values, of two stable states, which may be two equilibrium solutions (steady states) or two periodic solutions, or one equilibrium and one periodic solution. We demonstrate this observation with three types of models: 1) integrate-and-fire models, 2) Hopfield network models, and 3) Hodgkin-Huxley networks.

7.1 Multistability: integrate-and-fire model

The simplest model for RI that illustrates the interplay between τ and multistability is the integrate-and-fire model whose dynamics are shown in Fig-

ure 5a. This recurrent inhibitory loop involves a single excitatory neuron, E, and an inhibitory neuron, I [87]. The membrane potential, V, of E increases linearly at a rate, R, until it reaches the firing threshold, Π. When $V = \Pi$, E spikes and V is reset to the resting membrane potential, V_0. The period is $T = \Pi/R$. The spike generated by E excites I, which in turn after a time delay, τ, delivers an inhibitory post-synaptic potential (IPSP) to E. In general the effect of this IPSP will be to change the timing of the next spike generated by E by an amount δ, where δ is a function of the phase at which the IPSP arrives after E has fired. However, here we assume that δ is independent of the phase and hence the effect of the IPSP when $R > 0$ is to decrease V by an amount δ. This is equivalent to increasing the time that the next spike generated by E occurs by an amount δ. For simplicity we take $V_0 = 0$ and define the following dimensionless variables: $\tau^* = \tau/T$, $t^* = t/T$, $v^* = V/\Pi$, $\Delta = \delta/\Pi$, so that the dimensionless firing threshold, period and voltage growth rate are, respectively, $\Pi^* = 1, T^* = 1, R^* = \Pi^*/T^* = 1$. Dropping the asterisks we see that the dynamics of the recurrent loop depend only on two parameters, namely $\tau > 0$ and $\Delta \geq 0$. When $\tau < 1$, E spikes periodically with period $1 + \Delta$. This is because decreasing the membrane voltage by an amount Δ is equivalent to increasing the interspike interval by $1 + \Delta$.

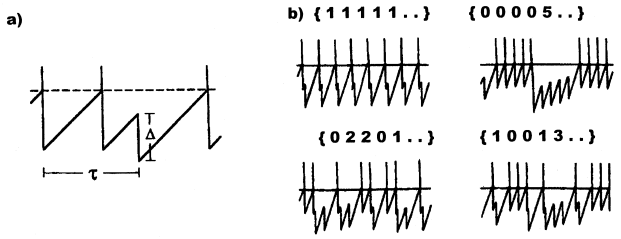

Fig. 5. a) The time course of the membrane potential v for the integrate-and-fire neuron E in a time-delayed RI. The dashed line indicates the threshold. b) Four co-existence periodic attractors that occur when $\tau = 4.1$ and $\Delta = 0.8$. The different patterns are described by the number of inhibitory pulses between two successive neuron spikings. Thus for the lower left pattern in b) we have going from left to right, 0 inhibitory pulses between the first two spikes, 2 inhibitory pulses between the next two spikes, then 2 inhibitory spikes, then 0, then 1. After this the pattern repeats. Thus the shorthand label for this spike pattern is {02201}.

The essential condition for multistability in this dimensionless model is that $\tau > 1$ (Figure 5b). Complex behaviors become possible since the inhibitory pulses are not necessarily the result of the immediately preceding excitatory pulse (Figure 5a). It can be shown that the solutions which arise can be constructed from segments of length τ, where each segment satisfies an equation of the form

$$\tau = x + m + x\Delta\,,$$

where m, n are positive integers and $0 < x < 1$. For τ, Δ fixed, the total numbers of pairs that satisfy this relationship is $\lceil \tau/\Delta \rceil$, where the notation $\lceil . \rceil$ denotes the smallest integer greater than τ/Δ. Since the number of (m, n) segments is finite for a given τ and Δ, it follows that all solutions are periodic with period $S(1 + \Delta)$ where S is the number of excitatory spikes per period.

Despite the simplicity of this mechanism for generating multistability, it makes a number of predictions that may be relevant for CAE. First, this model draws attention to the importance of the long recurrent loops associated with long τ's in generating paroxysmal events. For a given recurrent inhibitory loop, multistability can arise either because T is decreased or because τ is increased. Increasing the excitatory drive to cortex by, for example, up regulation of excitatory synapses, decreases T and hence would be expected to produce multistability (seizures) as is observed experimentally [88, 89]. On the other hand, brain maturation is associated with increased myelination of neuronal axons which increases their conduction velocities (see Section 8), thereby decreasing τ, and reducing the number of coexistent attractors. This observation could explain why this epilepsy is particularly common in children and why seizures tend to decrease in frequency, and even disappear altogether, as the child gets older.

7.2 Multistability: Hopfield model

The next step is to examine models which describe the dynamics of two interacting neurons. In particular we explore the dynamics exhibited by the motifs in Figure 4a using the equations for a Hopfield network. For 2-neuron circuit we have

$$\begin{aligned} \dot{x}_1 &= -k_1 x_1(t) + \omega_{11} g_{11}(x_1(t - \tau_{11})) + \omega_{21} g_{21}(x_2(t - \tau_{21})) + I_1\,, \\ \dot{x}_2 &= -k_2 x_2(t) + \omega_{22} g_{22}(x_2(t - \tau_{22})) + \omega_{12} g_{12}(x_1(t - \tau_{12})) + I_2\,. \end{aligned} \tag{4}$$

In this model, the variables $x_j(t)$ $(j = 1, 2)$ are the spiking rates of the neurons at time t and the k_j represent a natural decay of activity in the absence of input. The parameters ω_{ij} represent the strength of the connections: ω_{11} and ω_{22} are the strengths of the self-connections; ω_{12} is the synaptic weight from x_2 to x_1, ω_{21} is the weight from x_1 to x_2. The sign of ω_{ij} determines whether the synapse is excitatory $(\omega_{ij} > 0)$ or inhibitory $(\omega_{ij} < 0)$. The parameters I_j $(j = 1, 2)$ are the external inputs to the neurons. The function $g(x)$ is sigmoidal and can be written in many ways, most commonly taken as $\tanh(cx)$, $x^n/(c + x^n)$, or $1/(1 + e^{-cx})$. Appendices B and C illustrate applications of the use of readily available computer software packages for the analysis of (4).

The CI, RE and RI micro-circuits depicted in Figure 4a correspond to the following choices of signs in (4)

CI [12, 59, 61, 60, 90]: $\omega_{ij} < 0$
RE [90, 91, 92, 93, 94]: $\omega_{ij} > 0$
RI [87, 90, 95, 96, 97, 98, 99, 100]: $\omega_{11}, \omega_{12} < 0$, $\omega_{21}, \omega_{22} > 0$

The fixed point solutions of a system with time delays, $\bar{x}$, are the same as those of the corresponding system with zero delay. Thus for (4) we obtain $(\bar{x}_1, \bar{x}_2)$ by setting $\dot{x}_1 = \dot{x}_2 = 0$ and solving

$$0 = -k_1\bar{x}_1 + \omega_{11}g_{11}(\bar{x}_1) + \omega_{21}g_{21}(\bar{x}_2) + I_1\,, \tag{5a}$$
$$0 = -k_2\bar{x}_2 + \omega_{22}g_{22}(\bar{x}_2) + \omega_{12}g_{12}(\bar{x}_1) + I_2\,. \tag{5b}$$

Since our model is two dimensional, we can also visualize the determination of the fixed points geometrically (Figure 6). The fixed points are the intersection points of the curves defined by these equations. It is possible to analyze the equations in some detail to determine the number of possible equilibrium points see e.g. [101, 102].

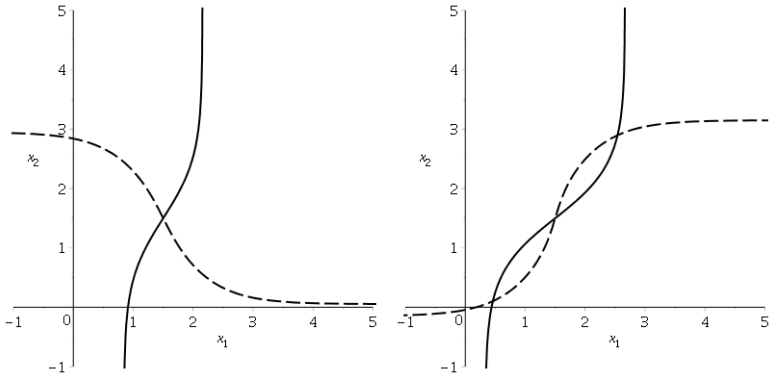

(a) RI circuit (b) RE circuit

Fig. 6. Nullclines showing single fixed point in RI case and multiple fixed points in RE case. The solid line gives the x_1-nullcline determined from (5a) and the dashed line gives the x_2-nullcline determined from (5b). The nonlinearity is $g_{ij}(u) = \tanh(u - \theta)$. Parameter values are (a) $\theta = 1.5, k_1 = 1, \omega_{11} = -0.6, \omega_{21} = 1, I_1 = 1.5, k_2 = 1, \omega_{12} = -1, \omega_{22} = 0.5, I_2 = 1.5$ and (b) $\theta = 1.5, k_1 = 1, \omega_{11} = 0.2, \omega_{21} = 1, I_1 = 1.5, k_2 = 1, \omega_{12} = 1, \omega_{22} = 0.7, I_2 = 1.5$.

To determine the stability of a fixed point we use linear stability analysis. First we linearize (4) about a fixed point, $\bar{x}$:

$$\dot{u}_1 = -k_1u_1(t) + a_{11}u_1(t - \tau_{11}) + a_{21}u_2(t - \tau_{21})\,, \tag{6}$$
$$\dot{u}_2 = -k_2u_2(t) + a_{22}u_2(t - \tau_{22}) + a_{12}u_1(t - \tau_{12})\,,$$

where $u(t) = x(t) - \bar{x}$ and $a_{ij} = \omega_{ij} g'_{ij}(\bar{x}_i)$. This model will tell us about the evolution of solutions which start *close enough* to a fixed point. To determine whether these solutions grow or decay in time, we consider trial solutions of the form $u \sim e^{\lambda t}$. Substituting this form into (6) and simplifying we arrive at the *characteristic equation*:

$$(\lambda + k_1 - a_{11}e^{-\lambda\tau_{11}})(\lambda + k_2 - a_{22}e^{-\lambda\tau_{22}}) - a_{12}a_{21}e^{-\lambda(\tau_{12}+\tau_{21})} = 0\,. \qquad (7)$$

Any root λ of this equation leads to a solution of (6). The roots may be real or complex. If all the roots have negative real parts then all solutions of (6) decay to zero in the longterm. In this case the fixed point of (4) is stable. If at least one root has positive real part the some solutions of (6) will grow in time. In this case the fixed point of (4) is unstable. If any root has zero real part then the stability is not determined by the linearization.

If there are no delays in the model, then (7) is a quadratic polynomial, and has two roots which can be explicitly determined. The presence of the delays means that there are *an infinite number* of roots. Nevertheless, mathematical analysis can be used to determine if the equilibrium point is stable or not. In particular, one can show that all the roots except a finite number (possibly zero) have negative real parts. Of particular interest is the fact that the delays associated with the connections between the neurons only appear in the combination $\tau_{12} + \tau_{21}$. Thus, for the motifs we are considering, it is the *total* delay of the loop that is important not the individual components, as is well-known [85]. Note that the parameter a_{11} depends explicitly on ω_{11} but may also depend implicitly on the other ω_{ij} through the value of the fixed point, $\bar{x}_1$. Similarly for the other a_{ij}. This can complicate the analysis.

Bifurcations can occur in the system when a change of stability of an equilibrium point occurs. From the discussion above this corresponds to the situation when at least one root of the characteristic equation has zero real part, and the rest have negative real parts. To begin we focus on the simplest case, when the characteristic equation has a zero root ($\lambda = 0$). This situation is associated with a bifurcation that *creates or destroys fixed points*, thus can be important in the generation of multistability of fixed points.

In the micro-circuit model this type of bifurcation can occur if

$$(k_1 - a_{11})(k_2 - a_{22}) - a_{12}a_{21} = 0\,. \qquad (8)$$

Recalling the definitions of the a_{ij} and the signs of the coupling, it is clear that this type of bifurcation is possible in all the micro-circuits, but only under some constraints for example:

CI $a_{12}\,a_{21}$ sufficiently large, i.e., strong enough coupling between neurons
RE $a_{11} > k_1$ and $a_{22} > k_2$ or $a_{11} < k_1$ and $a_{22} < k_2$, i.e., similar self-coupling on both neurons either strong or weak
RI $a_{22} > k_2$ i.e., strong enough self-coupling on the inhibitory neuron

The next and perhaps most important case is when the characteristic equation has a pair of pure imaginary roots Ωi. Setting $\lambda = \Omega i$ in (7) and separating pure and imaginary parts yield the pair of equations

$$k_1 k_2 - \Omega^2 + a_{11}a_{22}\cos(\Omega[\tau_{11}+\tau_{22}]) + a_{12}a_{21}\cos(\Omega[\tau_{12}+\tau_{21}]) - \Omega[a_{22}\sin(\Omega\tau_{22}) + a_{11}\sin(\Omega\tau_{11})] - k_1 a_{22}\cos(\Omega\tau_{22}) - k_2 a_{11}\cos(\Omega\tau_{11}) = 0\,, \quad (9)$$

$$(k_1+k_2)\Omega - a_{11}a_{22}\sin(\Omega[\tau_{11}+\tau_{22}]) + a_{12}a_{21}\sin(\Omega[\tau_{12}+\tau_{21}]) - \Omega[a_{22}\cos(\Omega\tau_{22}) + a_{11}\cos(\Omega\tau_{11})] - k_1 a_{22}\sin(\Omega\tau_{22}) + k_2 a_{11}\sin(\Omega\tau_{11}) = 0\,. \quad (10)$$

Fixing all the parameters except one, these equations can be solved for the value of the control parameter at which the pure imaginary roots occur and the corresponding value of Ω. Note that the equations are periodic with respect to each of the delays. Thus, fixing all of the parameters except one delay, say τ_{ij}, if $(\Omega^*,\ \tau_{ij}^*)$ is a solution of these equations, then $(\Omega^*,\ \tau_{ij}^* + 2m\pi/\Omega)$, are also solutions for any integer value of m.

Alternatively, equations (9)–(10) can be thought of as defining curves for two control parameters in terms of Ω and the other parameters. Figure 7 shows two examples where the control parameters are the combinations $\tau_{12}+\tau_{21}$ and $a_{12}a_{21}$.

Under appropriate conditions on the nonlinearities in the model (the functions g_{ij}) the system will undergo a *Hopf bifurcation* at these points, leading to the creation of a periodic solution. The stability of this solution also depends on the nonlinearities. See [43, 46, 103, 104, 105] for more details.

It is well known that the presence of delay in a model can facilitate the occurrence of Hopf bifurcations, this is known as a *delay-induced Hopf bifurcation*. In the micro-circuit model, it is straight forward to show that Hopf bifurcations are not possible if there are no delays (i.e. $\tau_{ij} = 0$) regardless of the signs of the connection weights.

More complex bifurcations can occur if the characteristic equation has multiple roots with zero real part. In models with delay it has been shown that such behavior is quite prevalent if the system has multiple delays [103, 106, 107]. Such points, which correspond to intersection points on the bifurcation curves shown in Figure 7, can lead to multistability and more complex dynamics [104, 105]. Examples of this behavior are illustrated in Figure 8.

We briefly outline some situations that can occur. If the characteristic equation has a double zero root (a Bogdanov-Takens bifurcation point), it is possible to have multistability between a slowly varying periodic solution and one or more fixed points. This has been shown to occur in the RI [108] and CI [85, 107] microcircuits. If the characteristic equation has a zero root and a pure imaginary pair it is possible to have multistability between a periodic solution and one or more fixed points. If the characteristic equation has two pairs of pure imaginary eigenvalues without resonance, then it is possible to have bistability between periodic orbits with an unstable two torus (or the reverse). This has been shown to occur in the CI and RI microcircuits [85, 107].

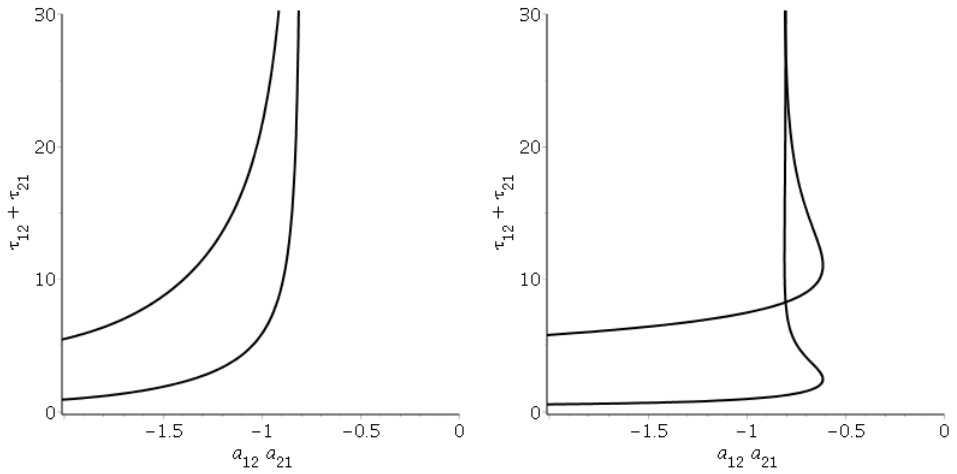

(a) $\tau_{11} = 1$ (b) $\tau_{11} = 3$

Fig. 7. Bifurcation curves for an RI circuit in connection strength-delay parameter space. The curves are determined by equations (9)–(10). Due to the periodicity with respect to $\tau_{12}+\tau_{21}$ in these equations, there is an infinite set of curves, of which two are shown. The parameter values for k_j, ω_{jj}, I_j, $j = 1, 2$ are given in Figure 6(a), $\tau_{22} = 0$ and τ_{11} as shown. When the delay in the local loop of the inhibitory neuron, τ_{11}, is large enough intersection points can occur. The fixed point is stable to the right of the curves.

Recalling our interpretation of this model in terms of firing rates, we can give biological meaning to these figures. For example, in Figure 8e the neurons are firing at some steady rate when a brief stimulus switches this to a large amplitude oscillatory firing rate. This spontaneously disappears after some time and the system settles on a (different) steady firing rate. The large amplitude oscillation correponds to an unstable periodic orbit, which is present due to the delay in the system. With no delay, the system merely switches between two different firing rates (Figure 8a). The oscillatory behaviour is sometimes referred to as a delayed induced transient oscillation (DITO). Our main point is that the DITO behaviour is very reminiscent of the seizure behaviour observed Figure 1.

7.3 Multistability: Hodgkin-Huxley models with delayed recurrent loops

The next step is examine the effects of the ion channels on the dynamics of delayed recurrent loops. Foss et al. [87] described the membrane potential of the excitatory neuron E using the following Hodgkin-Huxley model (HH) by considering the effect of IPSP as self-feedback

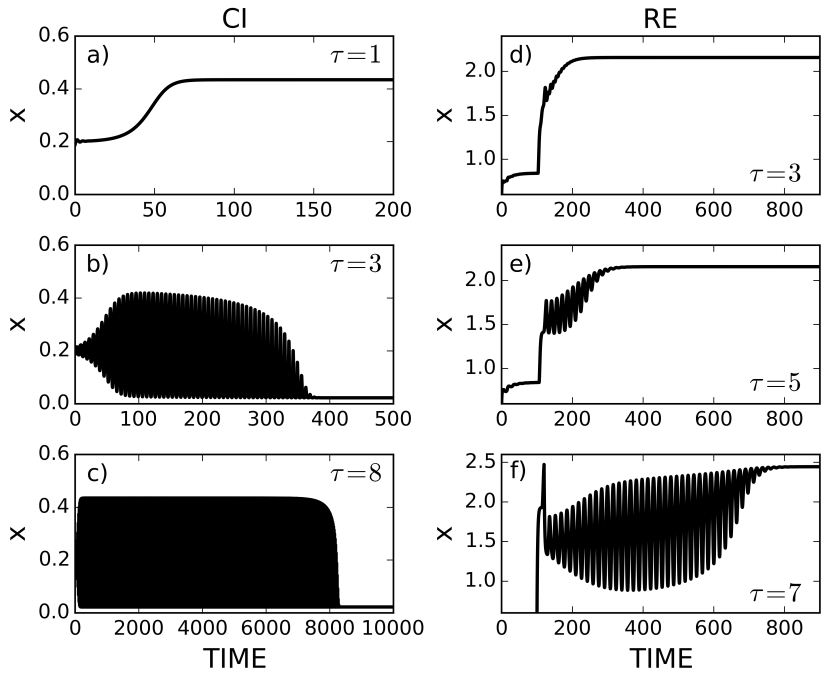

Fig. 8. Bistability between fixed points separated by an unstable limit cycle (DITO). a)-c) CI circuit. d)-f) RE circuit. Details of the CI circuit are given in [59] and the XPPAUT program `ditto.edo` can be downloaded from `faculty.jsd.claremont.edu/jmilton/Math_Lab_tool/Programs/XPPAUT`. The program and parameters for the RE circuit are given in Appendix B. The initial conditions are chosen to place the dynamics near the separatrix that separates the two co-existent stable fixed points. In each case we show only the activity of one of the neurons and $\tau = \tau_{12} = \tau_{21}$. Note that the duration of the DITO's is much longer than τ.

$$\begin{cases} Cx'(t) = -g_{Na}m^3h(x(t) - E_{Na}) - g_K n^4(x(t) - E_k) \\ \qquad\qquad -g_L(x(t) - E_L) - F(x(t-\tau)) + I_s(t), \\ m'(t) = \alpha_m(x)(1-m) - \beta_m(x)m, \\ n'(t) = \alpha_n(x)(1-n) - \beta_n(x)n, \\ h'(t) = \alpha_h(x)(1-h) - \beta_h(x)h\,, \end{cases} \tag{11}$$

where $F(x)$ is the signal function which describes the effect of the inhibitory neuron I on the membrane potential of the excitatory neuron E, and τ is the time lag. Other variables and parameters include the membrane potential ($x(t)$), the membrane capacitance (C), the stimulus (I_s). Constants g_{Na} and g_K are the maximum conductance of sodium and potassium ion channels, the constant g_L is the conductance of leakage channel, constants E_{Na}, E_K and

E_L are empirical parameters called the reversal potential. There are three (gating) variables (m, n, h) that describe the probability that a certain channel is open, and these variables evolve according to the aforementioned system of ordinary differential equations with functions α and β indexed by (m, n, h) appropriately. The initial function ϕ in the interval $[-\tau, 0]$ were assumed to have the form of neural spike trains. Namely, it is given by a sum of square pulse functions.

With sufficiently large I_s that makes the neuron fire successively, several coexisting periodic attractors were found [87, 102, 109] (Figure 9). Solutions starting from domains of attraction of these periodic solutions exhibit exotic transient behaviors but eventually become periodic.

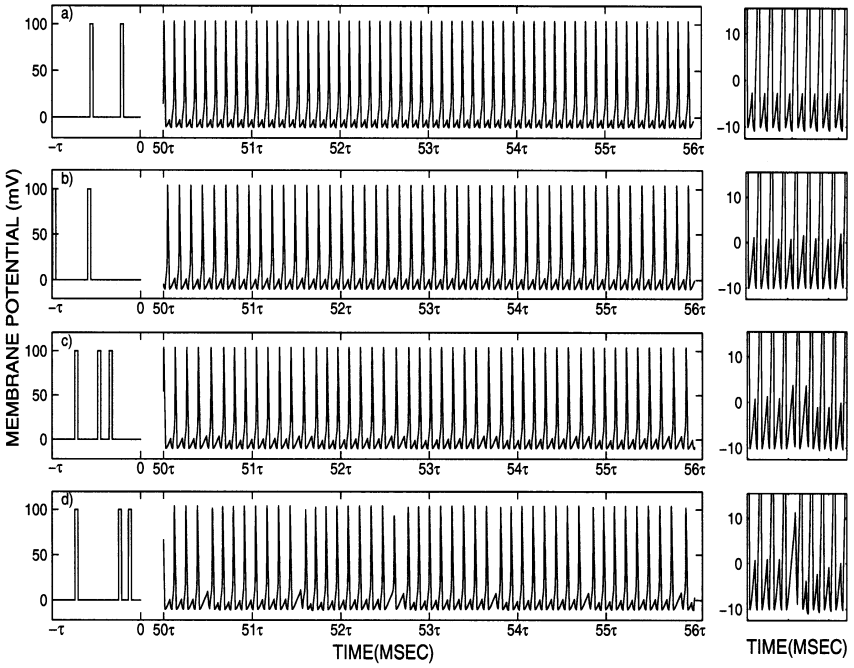

Fig. 9. Four coexisting attracting periodic solutions generated by the excitatory neuron E for the Hodgkin-Huxley model (HH) given by equations (11). The right-hand side is the blow up of the solutions in a given period (not delay τ) to clearly illustrate the patterns of solutions.

The corresponding linear integrate-and-fire model (LIF) and quadratic integrate-and-fire model (QIF) are given by

$$x'(t) = -\beta x(t) - F(x(t-\tau)) + I_s(t), \tag{12}$$
$$x'(t) = \beta(x-\mu)(x-\gamma) - F(x(t-\tau)) + I_s(t), \tag{13}$$

with the firing time t_f:

$$t_f : x(t) = \vartheta_1 \quad \text{and} \quad x'(t)|_{t=t_f} > 0,$$

and the firing threshold ϑ_1. These models can also exhibit multistability in terms of coexisting attractive periodic solutions, when the absolute refractoriness is incorporated. Each time the excitatory neuron fires a spike, a feedback is delivered at time τ later. The type of multistability not only depends on the time delay τ but also on the effective timing of the feedback impacting on the excitatory neuron. The total timing of the feedback is the portion of the duration when the spike is above the firing threshold. An important factor determining the effective timing of the feedback is the absolute refractory period, a short period after the firing of a spike during which the neuron is not affected by inputs at all. Systematic analysis can be conducted for both the linear integrate-and-fire model and quadratic integrate-and-fire model to determine when multistability occurs, how many coexisting attractive periodic solutions appear and their patterns (inter-spike intervals and oscillatory patterns within these intervals). See [102].

We note that multistability is also observed in RI models which take into account the phase resetting properties of each neuron in the loop [97, 110]. The advantage of this approach is that the phase resetting curve can be measured experimentally and thus all parameters in the model are known.

8 Developmental aspects

The developmental pattern of seizure recurrences in CAE suggests that there must be processes that are evolving on time scales of the order of years which modify the impact of the defect in the GABA_A on neurodynamics at a given age. There are two main changes that occur in the human brain between 3-4 years of age and adolescence.

First there are changes in synaptic density, namely the number of synapses per unit volume of cortical tissue [111, 112, 113]. At birth the infant brain has a synaptic density nearly equal to that of the adult brain [112]. Beginning within the first year of life there is a 30-40 % increase in synaptic density which peaks in the frontal cortex between ages 3-4 [113]. This is followed by a process of synaptic elimination so that by adolescence the synaptic density is again approximately equal to that of the adult.

Second, there are changes in axonal myelination and hence axonal conduction velocities. The active period for axonal myelination in the brain begins during the 28 week of gestation and then slows by mid to late adolescence. In some of the anterior association areas of the cortex, myelination continues until the 5th decade [114, 115]. The changes in myelination occur in a predictable

spatial and temporal sequence [115]. Myelination proceeds in a posterior to anterior direction so that sensory pathways myelinate first, followed by motor pathways and then the association areas. Within a given functional circuit, sub-cortical structures myelinate before cortical regions. The corpus callosum, the major white matter bundle connecting the two hemispheres, begins myelinating at 4 months post-natally and is not complete until mid to late adolescence: the anterior part is the last to myelinate. The time course for the disappearance of absence seizures in CAE coincides with the myelination of the long association and commissural fibers in the anterior quadrants of the brain. Thus the ages during which seizure activity is highest corresponds to the time when synapses are being eliminated from the brain and the myelination of axons is increasing. In particular the disappearance of absence seizures coincides with the myelination of the long association and commissural fibers in the anterior quadrants of the brain which connect different regions of cortex within the same hemisphere (association fibers) and between the two hemisphere (commissural fibers).

It is not known whether changes in synapses and/or changes in axonal conduction velocities are most important for expression of absence seizures in CAE. However, the observation that there are no long term cognitive impairments in CAE patients and the intelligence of children with CAE is within normal limits provided that their seizures are well controlled suggests that it is unlikely that seizure generation is related to abnormalities in synaptic density. On the other hand, with the advent of diffusion tensor imaging (DTI) techniques, abnormalities in myelination have been identified in children with CAE, particularly in the anterior part of the corpus callosum [116]. Similar abnormalities have been reported in a rat model for absence epilepsy [117]. Although these associations do not prove causality, they do suggest the possibility that the dependence of axonal conduction velocities (and hence time delays) on myelination might be an important parameter for this dynamic disease.

In a similar manner, the developmentally dependent changes related to τ may also explain the bimodal incidence of all types of epilepsy shown in Figure 10. Epileptic seizures are most common in the young and the elderly. Studies on aging monkeys suggest that increases in axonal conduction velocity are related to the death of oligodendrocyctes, namely the cell type responsible for myelinating axons in the brain. When an oligodendrocyte dies, other oligodendrocytes remyelinate the axon. However, the new myelin sheaths are thinner and the internode distances are shorter. Consequently, v is decreased and τ is increased.

Although the concept that the brain is most susceptible to generating seizures when τ is long is appealing, it may be an oversimplification. Indeed mean field estimates of cortical instability boundaries suggest that as v increases (τ decreases), the cortical model is able to reproduce SWDs [119].

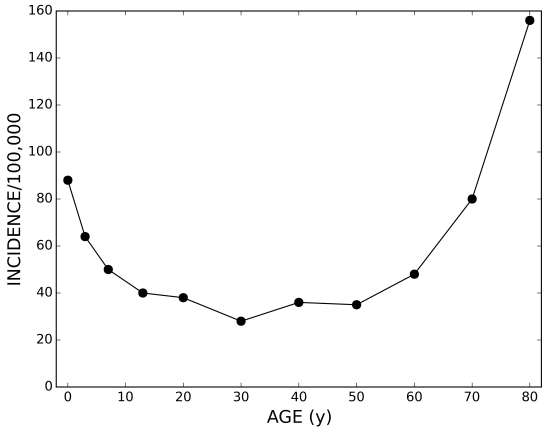

Fig. 10. Age-related incidence of epilepsy in industrialized societies. The data is from [118] and we have pooled data for males and females.

9 Discussion

The brain is a high-dimensional and complex dynamical system. The high dimensionality arises because the number of neurons is large and signals between them are time delayed. The dynamics of the microcircuit building blocks of the brain, such as CI, RE and RI, all exhibit multistability. Thus it is not surprising that many authors have emphasized metaphors for brain dynamics that take the form of potential landscapes with many "hills" and "valleys" [28, 67, 120, 121]. Moreover this landscape itself continually changes as a result of changes in states of arousal, aging, and as the brain learns and adapts to its environment [12, 122]. Frequent transitions between the attractors ("hills") lead to mesoscopic states in which dynamics are bounded and time-dependent. A lower bound for neurodynamics is ensured because excitatory connections exceed inhibitory ones and the upper bound is the result of neural refractoriness, accommodation and limited energy resources.

Our approach has emphasized that clinically significant changes in neurodynamics, such as the occurrence of an epileptic seizure, may be more related to the unstable states that separate attractors ("hills") than to the stable attractors [28, 47]. This concept can be most readily understood in the context of the DDEs that describe the microcircuits which generate DITOs [12, 59, 60, 61, 93]; however, DITO-like phenomena can also arise in other contexts as well [123]. A DDE corresponds to an infinite dimensional dynamical system since the number of initial conditions that must be specified to obtain a solution is infinite. Each initial condition is associated with an eigenvalue. For the unstable solution that separate two attractors, there must be at least one positive eigenvalue. This means that in the long time

the solutions must converge on one of the attractors. However, the short-time behaviors are influenced by the eigenvalues which have negative real parts. Consequently, the dynamical behaviors can be momentarily "trapped" in the vicinity of the unstable fixed-point. Our suggestion is that these "momentarily trapped" behaviors can sometimes be manifested as an epileptic seizure.

The study of the dynamics of neural microcircuits at the benchtop has a long history. Most often "hybrid" analogues of microcircuits are created in which a neuron interacts with an electronic device to collectively form a microcircuit (for a review see [124]). Modern day approaches use optogenetic techniques to manipulate neural microcircuits *in situ* [83]. However, it is not yet known how changes at the level of ion channels, e.g. the $\mathrm{GABA_A}$ receptor in CAE, result in episodic seizure recurrences. It is possible that this will become clear as we understand the rules that relate the dynamics of single microcircuit to those of large ensembles of microcircuits. In this way the study of CAE may not only bring relief to its sufferers and their families, but also provide insights into how the brain functions.

Acknowledgements We thank B. Fortini for useful discussions. JM was supported by the William R. Kenan Jr. Charitable Trust. JB, SAC and JW acknowledge support from the National Sciences and Engineering Research Council of Canada. JW received additional support from the Canada Research Chairs Program. JB received additional support from Fonds de recherche du Québec - Nature et technologies (FRQNT).

Appendix A: Numerical methods

Two numerical techniques which can aid in the study of delay differential equations such as (4),(11),(12) and (13) are numerical simulation and numerical bifurcation analysis.

Numerical simulation determines an approximate solution of a differential equation for a given choice of the initial state. Recall that for a delay differential equation, the initial state is a function which determines the value of the solution for t in $[-\tau, 0]$. For example, for the two-neuron Hopfield networks described by (4), the initial state is specified as follows

$$x_1(t) = \phi_1(t),\ x_2(t) = \phi_2(t), \quad -\tau \le t \le 0.$$

Typically ϕ_1, ϕ_2 are taken to be a constant, i.e.,

$$x_1(t) = x_{10},\ x_2(t) = x_{20}, \quad -\tau \le t \le 0\,,$$

which is reasonable for most experimental systems. It should be noted that only solutions which are stable can be accurately approximated using numerical simulation. The presence of unstable solutions may be deduced from

transient behavior, but details of the structure cannot be found through numerical simulation.

There are two commonly used programs for the numerical integration of delay differential equations. The free, stand-alone package XPPAUT [125] can perform numerical integration using a variety of fixed-step numerical methods. The program is run through a graphical user interface which is used not just to visualize results, but also to modify parameters, initial conditions and even the numerical integration method. The main benefit of this program is its flexibility and the ease with which different simulations can be compared. Information on how to download the package as well as documentation and tutorials are available at `www.math.pitt.edu/~bard/xpp/xpp.html`. The book [126] gives a overview of the package including many examples. XPPAUT code for the micro-circuit example (4) considered in this chapter is included in Appendix B. The MATLAB function, DDE23 [127], is a variable step size numerical integration routine for delay differential equations. A tutorial on this routine available at `www.mathworks.com/dde_tutorial` and the DDE23 code for the micro-circuit example in Appendix B is given in Appendix C. A benefit of using DDE23 is that results may be visualized using the extensive graphing tools of MATLAB.

Numerical bifurcation analysis has two aspects: the approximation of a solution and the calculation of the stability of this solution. The approximation of a solution done using numerical continuation, which uses a given solution for a particular parameter value to find a solution for a different (but close) parameter value. Numerical continuation can find both stable and unstable equilibrium and periodic solutions. More complex solutions (such as tori) are not implemented in all packages. Once the continuation has found an equilibrium solution to a desired accuracy, a numerical bifurcation program determines approximations for a finite set of the eigenvalues with the largest real part. The stability of periodic orbits can be numerically determined in a similar way. Numerical bifurcation packages generally track the stability of equilibrium points and periodic orbits, indicating where bifurcations occur.

One commonly used package that carries out numerical bifurcation analysis for delay differential equations is DDE-BIFTOOL [128], which runs in MATLAB. An overview of the numerical methods used in this package and some examples of applications can be found in [129]. The user manual and information on how to download the package are available at
`twr.cs.kuleuven.be/research/software/delay/ddebiftool.shtml`

A list of other software available for working with delay differential equations can be found at
`twr.cs.kuleuven.be/research/software/delay/software.shtml`

Appendix B: Delay differential equations using XPPAUT

Here we illustrate the use of XPPAUT for simulating the neural micro-circuits shown in Figure 4 using the Hopfield equations described by (4). Our focus is on how time delay differential equations (DDE) are handled in XPPAUT and how stimuli in the form of pulses can be used to cause switches between attractors.

In our experience installing XPPAUT on PC computers is quite straightforward. However, problems can arise when installing XPPAUT on Mac computers. The IT department at The Ohio State University has prepared a very useful installation guide for Mac users which can be accessed at

`https://docs.math.osu.edu/mac/how-tos/install-xpp-xppaut-mac/`

```
# Note: in ODE files, comments are preceded by #
#
# This program numerically integrates the
# Hopfield neural net equations with delay.
# We show the parameter choices for a RE circuit.
# However, the parameter choices we recommend for CI and  RI
# are given in Comments 3-4.  Note that the # command can be used
# to comment out lines of code which are not required.
#
# EQUATIONS

# See Comment 1

x1'= -k1*x1+w11*f1(delay(x1,tau11))+w21*f2(delay(x2,tau21))+I1+Istim1
x2'= -k2*x2+w12*f1(delay(x1,tau12))+w22*f2(delay(x2,tau22))+I2+Istim2
f1(x)=tanh(n1*(x-theta1))
f2(x)=tanh(n2*(x-theta2))

# See Comment 2

Istim1=I11*(heav(t-tstart1)-heav(t-tend1))
Istim2=I22*(heav(t-tstart2)-heav(t-tend2))

# PARAMETERS
# These parameters will reproduce Figure 8 b)

# See Comments 3, 4

p k1=1,k2=1
p w11=0.5,w21=1,w22=0.5,w12=0.5
p tau11=1,tau12=7,tau21=7,tau22=15
p n1=1,n2=1,theta1=1.5,theta2=1.5
```

```
p I1=1.5,I2=1.5
p I11=0.805,tstart1=100,tend1=120
p I22=0,tstart2=100,tend2=120

# INITIAL CONDITIONS

See Comment 5

init x1=0.5,x2=0.6
x1(0)=0.5
x2(0)=0.6

# CHANGES FROM XPP'S DEFAULT VALUES

# See Comment 6

@ total=400,dt=.01,xhi=400,maxstor=2000000,delay=10

done
```

Comments:

1. Terms of the form $x(t-\tau)$ become `delay(x,tau)` in XPPAUT. See also Comment 5.
2. Switches between co-existing attractors are made by using square pulses. The magnitude of the pulse is given by `I11,I22`. The onset of the pulse occurs at `tstart` and the end of the pulse occurs at `tend`.
3. Counter inhibition (CI). Make the following parameter changes to the RE program (above):

   ```
   w12=w21=-1.2
   w11=-0.1,w22=-0.2
   tau11=tau22=6, tau12=tau21=4.5
   I11=I22=1
   tstart1=tstart2=300
   tend1=tend2=320
   ```

   with the initial conditions:

   ```
   init x1=1,x2=2.1
   x1(0)=1
   x2(0)=2.1
   ```

   For these choices of the parameters, there are three coexisting attractors: two stable fixed points and a stable limit cycle. As the time delays `tau12,tau21` are decreased the limit cycle dusappears.
4. Recurrent inhibition (RI). Make the following parameter changes to the RE program (above):

```
w11=-0.6, w12=-1, w21=1, w22=0.5
tau11=3,tau12=4.5,tau21=4.5,tau22=0
I11=0.45, tstart1=450 tend1=470
I22=0
```

with the initial conditions:

```
init x1=2,x2=2.1
x1(0)=2
x2(0)=2.1
```

For these choices of the parameters, there is bistability between two limit cycles with an unstable torus in between. Changing the delays just a little eliminates the bistability.

5. In mathematics, the initial function, ϕ, for a DDE is defined on the interval $[-\tau, 0]$. However, in XPPAUT ϕ is divided into two parts: the initial condition at t=0, $\phi(0)$, and a function $\phi(s)$ where $s \in [-\tau, 0)$. The default choice is $\phi(s) = 0$. The commands `x1(0)=0.1` and `x2(0)=0.2` set $\phi(s)$ to a constant value. A look up table can be used to introduce an arbitrary $\phi(s)$ as shown in [59]. In running a XPPAUT program for a DDE it is necessary to open three windows `Initial Data`, `Delay ICs` and `Parameters`. The `Initial Data` panel will show the initial data, the `Delay ICs` will show $\phi(s)$ and the `Parameters` panel will show the parameter choices to be used for the simulation. An important point is that to run the simulation one must click on 'OK' for each panel and then click on 'Go' on one of these panels. Failure to do this will result in numerical errors since the initial function will not be handled correctly. Finally when determining the nullclines it is important to set all of the delays to 0.
6. The parameter `delay` should be greater than `tau`. The parameter `delay` reserves the amount of memory needed to store ϕ for each variable. Since one of the goals of the simulation is to see the effect of changing τ on the dynamics, it is convenient to set `delay` slightly higher that the largest delay anticipated. If the program runs out of memory, the amount of memory reserved for this purpose can be increased by using the command `maxstor`.

Appendix C: Delay differential equations using Matlab's dde23

For users that have access to the latest version of Matlab, it is possible to integrate the Hopfield equations described by (4) using `dde23`. Here we give the code that integrates the RE model for the same parameters as described above. Note that two m files are required: `delay_circuit.m` supplies the parameters and performs the integration; `DRHS.m` gives the equations to be integrated. The symbol `%` comments out the parts of the code that are not

needed for the RE circuit. In order to run this program, put both files in the same directory and then type `delay_circuit()`

DRHS.m

```
function yp = DRHS(t,y,Z);

global k W n theta I Istim tstart tend;

% Z(i,j) = xi(t-tauj)
% tau=[tau11,tau12,tau21,tau22]
ylag11 = Z(1,1); % x1(t-tau11)
ylag12 = Z(1,2); % x1(t-tau12)
ylag21 = Z(2,3); % x2(t-tau21)
ylag22 = Z(2,4); % x2(t-tau22)
yp = [
-k(1)*y(1) + W(1,1)*tanh(n(1)*(ylag11-theta(1))) ...
+ W(2,1)*tanh(n(2)*(ylag21-theta(2))) ...
+ I(1) + Istim(1)*(heaviside(t-tstart(1))-heaviside(t-tend(1)));
-k(2)*y(2) + W(1,2)*tanh(n(1)*(ylag12-theta(1))) ...
+ W(2,2)*tanh(n(2)*(ylag22-theta(2))) ...
+ I(2) + Istim(2)*(heaviside(t-tstart(2))-heaviside(t-tend(2)));
];
```

Note: The entries for `yp` are very long. The `...` is the Matlab code for breaking up long equations into shorter ones.

delay_circuit.m

```
function delay_circuit()
clear all;
close all;
clc;
global tau;
global k W n theta I Istim tstart tend;

% Initialization
% delays
tau11=0.001;
tau22=15;

% other parameters
w11=0.5;
w21=1;
w12=0.5;
```

```
w22=0.5;
theta=[1.5,1.5]';
I=[1.5,1.5]';
n=[1,1]';
k=[1,1]';

% stimulation parameters
I11=0.805;
tstart1=100;
tend1=120;
I22=0;
tstart2=100;
tend2=120;

% initial conditions
y10=0.5;
y20=0.6;

% start/end values of t
t0=0;
t1=1000;

% min/max for plotting
umin = 0;
umax = 3;

% matrix form of parameters
W=[[w11,w21]',[w12,w22]']
Istim=[I11,I22]'
tstart=[tstart1,tstart2]'
tend=[tend1,tend2]'
% initial conditions
yi =[y10,y20]'
% integration time
interval=[t0, t1];

% First plot
tau=[tau11, 1., 1., tau22]
sol = dde23('DRHS',tau,yi,interval);
fig1 = figure(1);
subplot(3,1,1);
plot(sol.x,sol.y(2,:),'-b','LineWidth',2);
title('\tau_{12}=\tau_{21}=1');
xlabel('time t');
ylabel('x_2(t)');
```

```
axis([t0 t1 umin umax]);
grid on;

% Second plot
tau=[tau11, 6., 6., tau22]
sol = dde23('DRHS',tau,yi,interval);
subplot(3,1,2);
plot(sol.x,sol.y(2,:),'-b','LineWidth',2);
title('\tau_{12}=\tau_{21}=6');
xlabel('time t');
ylabel('x_2(t)');
axis([t0 t1 umin umax]);
grid on;

% Third plot
tau=[tau11, 7., 7., tau22]
sol = dde23('DRHS',tau,yi,interval);
subplot(3,1,3);
plot(sol.x,sol.y(2,:),'-b','LineWidth',2);
title('\tau_{12}=\tau_{21}=7');
xlabel('time t');
ylabel('x_2(t)');
axis([t0 t1 umin umax]);
grid on;

end
```

References

1. L. Glass and M. C. Mackey. Pathological conditions resulting from instabilities in physiological control systems. *Ann. New York Acad. Sci.*, 316:214–235, 1979.
2. M. C. Mackey and L. Glass. Oscillation and chaos in physiological control systems. *Science*, 197:287–289, 1977.
3. M. C. Mackey and J. G. Milton. Dynamical diseases. *Ann. New York Acad. Sci.*, 504:16–32, 1987.
4. H. O. Lüders. *Deep brain stimulation and epilepsy.* Martin Dunitz, New York, 2004.
5. J. Milton and P. Jung. *Epilepsy as a dynamic disease.* Springer, New York, 2003.
6. I. Osorio and M. G. Frei. Real-time detection, quantification, warning and control of epileptic seizures: The foundation of a scientific epileptology. *Epil. Behav.*, 16:391–396, 2009.
7. I. Osorio, M. G. Frei, S. Sunderam, J. Giftakis, N. C. Bhavaraja, S. F. Schnaffer, and S. B. Wilkinson. Automated seizure abatement in humans using electrical stimulation. *Ann. Neurol.*, 57:258–268, 2005.

8. I. Osorio, M. G. Frei, and S. B. Wilkinson. Real-time automated detection and quantitative analysis of seizures and short-term prediction of clinical onset. *Epilepsia*, 39:615–627, 1998.
9. T. S. Salam, J. L. Perez-Velazquez, and R. Genov. Seizure suppression efficacy of closed-loop versus open-loop deep brain stimulation in a rodent model of epilepsy. *IEEE Trans. Neural Sys. Rehab. Eng.*, in press:xx, 2016.
10. G. Milton J, A. R. Quan, and I. Osorio. Nocturnal frontal lobe epilepsy: Metastability in a dynamic disease? In I. Osorio, H. P. Zaveri, M. G. Frei, and S. Arthurs, editors, *Epilepsy: The intersection of neurosciences, biology, mathematics, engineering and physics*, pages 501–510, New York, 2011. CRC Press.
11. I. Osorio, H. P. Zaveri, M. G. Frei, and S. Arthurs. *Epilepsy: The intersection of neurosciences, biology, mathematics, engineering and physics*. CRC Press, New York, 2011.
12. A. Quan, I. Osorio, T. Ohira, and J. Milton. Vulnerability to paroxysmal oscillations in delay neural networks: A basis for nocturnal frontal lobe epilepsy? *Chaos*, 21:047512, 2011.
13. J. Milton and D. Black. Dynamic diseases in neurology and psychiatry. *Chaos*, 5:8–13, 1995.
14. J. M. Rommens, M. L. Iannuzzi, B. Kerem, M. L. Drumm, G. Melmer, M. Dean, R. Rozmahel, J. L. Cole, D. Kennedy, and N. Hidaka. Identification of the cystic fibrosis gene: chromosome walking and jumping. *Science*, 245:1059–1055, 1989.
15. S. Coombes and P. C. Bressloff. *Bursting: The genesis of rhythm in the nervous system*. World Scientific, New Jersey, 2005.
16. G. B. Ermentrout and D. H. Terman. *Mathematical Foundations of Neuroscience*. Springer, New York, 2010.
17. W. Gerstner and W. Kistler. *Spiking neuron models: single neurons, populations, plasticity*. Cambridge University Press, New York, 2006.
18. E. M. Izhikevich. *Dynamical systems in neuroscience: The geometry of excitability and bursting*. MIT Press, Cambrdige, MA, 2007.
19. C. Koch and I. Segev. *Methods in Neuronal Modeling: From synapses to networks*. MIT Press, Cambridge, Ma, 1989.
20. J. Rinzel and G. B. Ermentrout. Analysis of neural excitability and oscillations. In C. Koch and I. Segev, editors, *Methods in Neuronal Modeling: From synapses to networks*, pages 135–169, Cambridge, MA, 1989. MIT Press.
21. J-B. Kim. Channelopathies. *Korean J. Pediatr.*, 57:1–18, 2013.
22. D. M. Kullman and S. G. Waxman. Neurological channelopathies: new insights into disease mechanisms and ion channel function. *J. Physiol.*, 588.11:1823–1827, 2010.
23. E. Sigel and M. E. Steinman. Structure, function and modulation of $GABA_a$ receptors. *J. Biol. Chem.*, 287:40224–40231, 2012.
24. P. Gloor, M. Avoli, and G. Kostopoulos. Thalamo-cortical relationships in generalized epilepsy with bilaterally synchronous spike-and-wave discharge. In M. Avoli, P. Gloor, R. Naquet, and G. Kostopoulos, editors, *Generalized Epilepsy: Neurobiological Approaches*, pages 190–212, Boston, 1990. Birkhäuser.
25. G. K. Kostopoulos. Spike-and-wave discharges of absence seizures as a transformation of sleep spindles: the continuing development of a hypothesis. *Clin. Neurophysiol.*, 111 (S2):S27–S38, 2000.

26. L. Cocito and A. Primavera. Vigabatrin aggravates absences and absence status. *Neurology*, 51:1519–1520, 1998.
27. S. Knack, H. M. Hamer, U. Schomberg, W. H. Oertel, and F. Rosenow. Tiagabine-induced absence status in idiopathic generalized nonconvulsive epilepsy. *Seizure*, 8:314–317, 1999.
28. J. G. Milton. Epilepsy: Multistability in a dynamic disease. In J. Walleczek, editor, *Self-organized biological dynamics and nonlinear control*, pages 374–386, New York, 2000. Cambridge University Press.
29. G. van Luijtelaar, C. Behr, and M. Avoli. Is there such a thing as "generalized" epilepsy? In H. E. Scharfman and P. S. Buckmaster, editors, *Issues in Clinical Epileptology: A View from the Bench*, pages 81–91, New York, 2014. Springer.
30. G. van Luijtelaar and E. Sitnikova. Global and focal aspects of absence epilepsy: The contribution of genetic models. *Neurosci. Biobehav. Rev.*, 30:983–1003, 2006.
31. J. Milton. Insights into seizure propagation from axonal conduction times. In J. Milton and P. Jung, editors, *Epilepsy as a dynamic disease*, pages 15–23, New York, 2003. Springer.
32. J. Bancaud. Physiopathogenesis of generalized epilepsies of organic nature (Stereoencephalographic study). In H. Gastaut, H. H. Jasper, J. Bancaud, and A. Waltregny, editors, *The Physiopathogenesis of the Epilepsies*, pages 158–185, Spingfield, Il, 1969. Charles C. Thomas.
33. J. Bancaud. Role of the cerebral cortex in (generalized) epilepsy of organic origin. Contribution of stereoelectroencephalographic investigations (S. E. E. G.) to discussion of the centroencephalographic concept. *Presse Med.*, 79:669–673, 1971.
34. H. K. M. Meeren, J. P. M. Pijn, E. L. J. M. Can Luijtelaar, A. M. L. Coenen, and F. H. Lopes da Silva. Cortical focus drives widespread corticothalamic networks during spontaneous absence seizures in rats. *J. Neurosci.*, 22:1480–1495, 2002.
35. D. Gupta, P. Ossenblok, and G. van Luijtelaar. Space-time network connectivity and cortical activations preceding spike wave discharges in human absence epilepsy: a MEG study. *Med. Biol. Eng. Comput.*, 49:555–565, 2011.
36. J. R. Tenney, H. Fujiwara, P. S. Horn, S. E. Jacobsen, T. A. Glaser, and D. F. Rose. Focal corticothalamic sources during generalized absence seizures: a MEG study. *Epilepsy Res.*, 106:113–122, 2013.
37. I. Westmije, P. Ossenblok, B. Gunning, and G. van Luijtelaar. Onset and propagation of spike and slow wave discharges in human absence epilepsy: a MEG study. *Epilepsia*, 50:2538–2548, 2009.
38. S. A. Chkhenkeli and J. Milton. Dynamic epileptic systems versus static epileptic foci. In J. Milton and P. Jung, editors, *Epilepsy as a dynamic disease*, pages 25–36, New York, 2003. Springer.
39. J. G. Milton, S. A. Chkhenkeli, and V. L. Towle. Brain connectivity and the spread of epileptic seizures. In V. K. Jirsa and A. R. McIntosh, editors, *Handbook of Brain Connectivity*, pages 478–503, New York, 2007. Springer.
40. M. Abeles, E. Vaadia, and H. Bergman. Firing patterns of single units in the prefrontal cortex and neural network models. *Network*, 1:13–25, 1990.
41. P. Lennie. The cost of cortical computation. *Current Biol.*, 13:493–497, 2003.
42. V.B. Kolmanovskii and V.R. Nosov. *Stability of functional differential equations*, volume 180 of *Mathematics in Science and Engineering*. Academic Press, London, England, 1986.

43. H. Smith. *An introduction to delay differential equations with applications to the life sciences*, volume 57. Springer Science & Business Media, 2010.
44. G. Stépán. *Retarded Dynamical Systems: Stability and Characteristic Functions*, volume 210 of *Pitman Research Notes in Mathematics*. Longman Group, Essex, 1989.
45. O. Diekmann, S. A. van Gils, S.M. Verduyn Lunel, and H.-O. Walther. *Delay Equations*. Springer-Verlag, New York, 1995.
46. J.K. Hale and S.M. Verduyn-Lunel. *Introduction to Functional Differential Equations*. Springer Verlag, New York, 1993.
47. F. H. Lopes da Silva, W. Blanes, S. Kalitizin, J. Parra Gomez, P. Suffczynski, and F. J. Velis. Epilepsies as dynamical diseases of brain systems: basic models of the transition between normal and epileptic activity. *Epilepsia*, 44 (suppl. 12):72–83, 2002.
48. C. M. Florez, R. J. McGinn, V. Lukankin, I. Marwa, S. Sugumar, J. Dian, .-N. Hazrati, P. L. Carlen, and L. Zhang. In vitro recordings of human neocortical oscillations. *Cerebral Cortex*, 25:578–597, 2015.
49. A. Destexhe. Spike-and-wave oscillations based on the properties of $GABA_B$ receptors. *J. Neurosci.*, 18:9099–9111, 1998.
50. A. Destexhe. Corticothalamic feedback: A key to explain absence seizures. In I. Soltesz and K. Staley, editors, *Computational Neuroscience in Epilepsy*, pages 184–214, San Diego, 2008. Academic Press.
51. A. B. Holt and T. I. Netoff. Computational modeling of epilepsy for an experimental neurologist. *Exp. Neurol.*, 244:75–86, 2013.
52. W. W. Lytton. Computer modeling of epilepsy. *Nat. Rev. Neurosci.*, 9:626–637, 2008.
53. I. Soltesz and K. Staley. *Computational Neuroscience in Epilepsy*. Academic Press, San Diego, 2008.
54. G. Baier and J. Milton. Dynamic diseases of the brain. In D. Jaeger and R. Jung, editors, *Encyclopedia of Computational Neuroscience*, pages 1051–1061, New York, 2015. Springer.
55. L. Glass. Dynamical disease: challenges for nonlinear dynamics and medicine. *Chaos*, 25:097603, 2015.
56. C. Foley and M. C. Mackey. Mathematical model for G-CSF administration after chemotherapy. *J. Theoret. Biol.*, 19:25–52, 2009.
57. M. C. Mackey. Periodic auto-immune hemolytic anemia: An induced dynamical disease. *Bull. Math. Biol.*, 41:829–834, 1979.
58. J. S. Orr, J. Kirk, K. G. Gary, and J. R. Anderson. A study of the interdependence of red cell and bone marrow stem cell populations. *Brit. J. Haematol.*, 15:23–34, 1968.
59. J. Milton, P. Naik, C. Chan, and S. A. Campbell. Indecision in neural decision making models. *Math. Model. Nat. Phenom.*, 5:125–145, 2010.
60. K. Pakdaman, C. Grotta-Ragazzo, and C. P. Malta. Transient regime duration in continuous-time neural networks with delay. *Phys. Rev. E*, 58:3623–3627, 1998.
61. K. Pakdaman, C. Grotta-Ragazzo, C. P. Malta, O. Arino, and J. F. Vibert. Effect of delay on the boundary of the basin of attraction in a system of two neurons. *Neural Netw.*, 11:509–519, 1998.
62. C. Beaulieu, Z. Kisvarday, P. Somoygi, M. Cynader, and A. Cowey. Quantitative distribution of GABA-immunoresponsive and -immunonegative neurons

and synapses in the monkey striate cortex (area 17). *Cerebral Cortex*, 2:295–309, 1992.
63. J. G. Milton. Epilepsy as a dynamic disease: A tutorial of the past with an eye to the future. *Epil. Beh.*, 18:33–44, 2010.
64. I. Osorio, M. G. Frei, D. Sornette, J. Milton, and Y-C. Lai. Epileptic seizures: Quakes of the brain? *Phys. Rev. E*, 82:021919, 2010.
65. G. A. Worrell, C. A. Stephen, S. D. Cranstoun, B. Litt, and J. Echauz. Evidence for self-organized criticality in human epileptic hippocampus. *NeuroReport*, 13:2017–2021, 2010.
66. M. Stead, M. Bower, B. H. Brinkmann, K. Lee, W. R. Marsh, F. B. Meyer, B. Litt, J. Van Gompel, and G. A. Worrell. Microseizures and the spatiotemporal scales of human partial epilepsy. *Brain*, 133:2789–2797, 2010.
67. J. Milton. Neuronal avalanches, epileptic quakes and other transient forms of neurodynamics. *Eur. J. Neurosci.*, 36:2156–2163, 2012.
68. W. Horsthemke and R. Lefever. *Noise-induced transitions: Theory and applications in physics, chemistry and biology*. Springer, New York, 1984.
69. P. Milanowski and P. Suffcznski. Critical transitions in epileptic systems. *Int. J. Neural Sys.*, in press:xx, 2016.
70. D. A. Williams. A study of thalamic and cortical rhythms in Petit Mal. *Brain*, 76:50–59, 1953.
71. M. Steriade. The GABAergic reticular nucleus: a preferential target of corticothalamic projections. *Proc. Natl. Acad. Sci. USA*, 98:3625–3627, 2001.
72. M. Steriade and D. Contreras. Relations between cortical and cellular events during transition from sleep patterns to paroxysmal activity. *J. Neurosci.*, 15:623–642, 1995.
73. M. J. Gallagher. How deactivating an inhibitor causes absence epilepsy: Validation of a noble lie. *Epilepsy Curr.*, 13:38–41, 2013.
74. E. G. Jones. *The Thalamus*. Plenum Press, New York, 1985.
75. C. Ajmone-Marsan. The thalamus. Data on its functional anatomy and on some aspects of thalamo-cortical organization. *Arch. Italiennes Biol.*, 103:847–882, 1965.
76. Y. Choe. The role of temporal parameters in a thalamocortical model of analogy. *IEEE Trans. Neural Netw.*, 15:1071–1082, 2004.
77. T. Tsumoto, O. D. Creutzfield, and C. R. Legendy. Functional organization of the corticofugal system from visual cortex to lateral geniculate nucleus in the cat. *Exp. Brain Res.*, 32:345–364, 1978.
78. C. E. Landisman, M. A. Long, M. Beierlein, M. R. Deans, D. L. Paul, and B. W. Connors. Electrical synapses in the thalamic reticular nucleus. *J. Neurosci.*, 22:1002–1009, 2002.
79. S-C. Lee, S. L. Patrick, K. A. Richardson, and B. W. Connors. Two functionally distinct networks of gap junction-coupled inhibitory neurons in the thalamic reticular nucleus. *J. Neurosci.*, 34:13170–12182, 2014.
80. J. G. Milton. *Dynamics of small neural populations*. American Mathematical Society, Providence, RI, 1996.
81. J. T. Paz and J. R. Huguenard. Microcircuits and their interactions in epilepsy: is the focus out of focus? *Nat. Neurosci.*, 18:351–359, 2015.
82. O. Sporns and R. Kötter. Motifs in brain networks. *PLoS Biol.*, 2:e369, 2004.
83. J. T. Paz, A. S. Bryant, K. Peng, L. Fenno, O. Yizhar, W. N. Frankel, K. Deisseroth, and J. R. Huguenard. A new mode of corticothalamic transmission

revealed in the Gria4-/- model of absence epilepsy. *Nat. Neurosci.*, 14:1167–1173, 2011.
84. A. M. Large, N. W. Vogles, S. Mielo, and A-M. M. Oswald. Balanced feedfoward inhibition and dominant recurrent inhibition in olfactory cortex. *Proc. Natl. Acad. Sci. USA*, 113:2276–2281, 2016.
85. S.A. Campbell. Stability and bifurcation of a simple neural network with multiple time delays. In S. Ruan, G.S.K. Wolkowicz, and J. Wu, editors, *Fields Inst. Commun*, volume 21, pages 65–79. AMS, 1999.
86. A. Payeur, L. Maler, and A. Longtin. Oscillatory-like behavior in feedforward neuronal networks. *Phys. Rev. E*, 92:012703, 2015.
87. J. Foss, A. Longtin, B. Mensour, and J. Milton. Multistability and delayed recurrent feedback. *Phys. Rev. Lett.*, 76:708–711, 1996.
88. K. D. Graber and D. A. Prince. A critical period for prevention of post-traumatic neocortical hyperexcitability in rats. *Ann. Neurol.*, 55:860–870, 2004.
89. A. R. Houweling, M. M. Bazhenov, I. Timofeev, M. Steraide, and T. J. Sejnowski. Homeostatic synaptic plasticity can explain post-traumatic epileptogenesis in chronically isolated neocortex. *Cerebral Cortex*, 15:834–845, 2005.
90. K. L. Babcock and R. M. Westervelt. Dynamics of simple electronic networks. *Physica D*, 28:305–316, 1987.
91. N. Azmy, E. Boussard, J. F. Vibert, and K. Pakdaman. Single neuron with recurrent excitation: Effect of the transmission delay. *Neural Netw.*, 9:797–818, 1996.
92. O. Diez Martinez and J. P. Segundo. Behavior of a single neuron in a recurrent excitatory loop. *Biol. Cybern.*, 47:33–41, 1983.
93. K. Pakdaman, J-F. Vibert, E. Boussard, and N. Azmy. Single neuron with recurrent excitation: Effect of the transmission delay. *Neural Netw.*, 9:797–818, 1996.
94. K. Pakdaman, F. Alvarez, J. P. Segundo, O. Diez-Martinez, and J-F. Vibert. Adaptation prevents discharge saturation in models of single neurons with recurrent excitation. *Int. J. Mod. Simul.*, 22:260–265, 2002.
95. Y. Chen and J. Wu. Slowly oscillating periodic solutions for a delayed frustrated network of two neurons. *J. Math. Anal. Appl.*, 259:188–208, 2001.
96. J. Foss, F. Moss, and J. Milton. Noise, multistability and delayed recurrent loops. *Phys. Rev. E*, 55:4536–4543, 1997.
97. J. Foss and J. Milton. Multistability in recurrent neural loops arising from delay. *J. Neurophysiol.*, 84:975–985, 2000.
98. M. C. Mackey and U. an der Heiden. The dynamics of recurrent inhibition. *J. Math. Biol.*, 19:211–225, 1984.
99. L. H. A. Monteiro, A. Pellizari Filho, J. G. Chaui-Berlinck, and J. R. C. Piquiera. Oscillation death in a two-neuron network with delay in a self-connection. *J. Biol. Sci.*, 15:49–61, 2007.
100. R. E. Plant. A Fitzhugh differential-difference equation modeling recurrent neural feedback. *SIAM J. Appl. Math.*, 40:150–162, 1981.
101. H.R. Wilson and J.D. Cowan. Excitatory and inhibitory interactions in localized populations of model neurons. *Biophys. J.*, 12(1):1, 1972.
102. J. Ma and J. Wu. Multistability in spiking neuron models of delayed recurrent inhibitory loops. *Neural Comp.*, 19:2124–2148, 2007.
103. J. Bélair and S.A. Campbell. Stability and bifurcations of equilibria in a multiple-delayed differential equation. *SIAM J. Appl. Math.*, 54(5):1402–1424, 1994.

104. J. Guckenheimer and P.J. Holmes. *Nonlinear Oscillations, Dynamical Systems and Bifurcations of Vector Fields*. Springer-Verlag, New York, 1983.
105. Y.A. Kuznetsov. *Elements of Applied Bifurcation Theory*, volume 112 of *Applied Mathematical Sciences*. Springer-Verlag, Berlin/New York, 1995.
106. S.A. Campbell, J. Bélair, T. Ohira, and J. Milton. Limit cycles, tori, and complex dynamics in a second-order differential equation with delayed negative feedback. *J. Dyn. Diff. Eqns.*, 7(1):213–236, 1995.
107. L. P. Shayer and S.A. Campbell. Stability, bifurcation, and multistability in a system of two coupled neurons with multiple time delays. *SIAM J. Appl. Math.*, 61(2):673–700, 2000.
108. G. Fan, S.A. Campbell, G.S.K. Wolkowicz, and H. Zhu. The bifurcation study of 1:2 resonance in a delayed system of two coupled neurons. *J. Dyn. Diff. Eqns.*, 25(1):193–216, 2013.
109. J. Ma and J. Wu. Patterns, memory and periodicity in two-neuron recurrent inhibitory loops. *Math. Model. Nat. Phenom.*, 5:67–99, 2010.
110. M. Timme and F. Wolf. The simplest problem in the collective dynamics of neural networks: Is synchrony stable? *Nonlinearity*, 21:1579–1599, 2008.
111. H. T. Chugani, M. E. Phelps, and J. C. Mazziotta. Positron emission tomography study of human brain function development. *Ann. Neurol.*, 22:487–497, 1987.
112. P. R. Huttenlocher. Developmental changes of aging. *Brain Res.*, 163:195–205, 1979.
113. P. R. Huttenlocher and A. S. Dabholkar. Regional differences in synaptogenesis in human cerebral cortex. *J. Comp. Neurol.*, 387:167–178, 1997.
114. N. Barnea-Goraly, V. Menon, M. Eckart, L. Tamm, R. Bammer, A. Karchemskiy, C. C. Dant, and A. L. Reiss. White matter development during childhood and adolescence: A cross-sectional diffusion tensor imaging study. *Cerebral Cortex*, 15:1848–1854, 2005.
115. G. Z. Tau and B. S. Peterson. Normal development of brain circuits. *Neuropschopharmacology*, 35:147–168, 2010.
116. J-S Liang, S-P Lee, B. Pulli, J. W. Chen, S-C Kao, Y-K Tsang, and K. L-C Hsieh. Microstructural changes in absence seizure children: A diffusion tensor magnetic resonance imaging study. *Ped. Neonatology*, in press:xx–xx, 2015.
117. H. Chahboune, A. M. Mishra, M. N. DeSalvo, L. H. Stocib, M. Purcano, D. Scheinost, X. Papademetris, S. J. Fyson, M. L. Lorincz, V. Crunelli, F. Hyder, and H. Blumenfeld. DTI abnormalities in anterior corpus callosum of rats with spike-wave epilepsy. *NeuroImage*, 47:459–466, 2009.
118. W. A. Hauser, J. F. Annegers, and L. T. Kurland. The incidence of epilepsy in Rochester, Minnesota, 1935-1984. *Epilepsia*, 34:453–468, 1993.
119. P. A. Robinson, C. J. Rennie, and D. L. Rowe. Dynamics of large-scale brain activity in normal arousal states and epileptic seizures. *Phys. Rev. E*, 65:041924, 2002.
120. W. J. Freeman. *Neurodynamics: An exploration of mesoscopic brain dynamics*. Springer Verlag, London, 2000.
121. W. J. Freeman and M. D. Holmes. Metastability, instability, and state transitions in cortex. *Neural Netw.*, 18:497–504, 2005.
122. E. Sitnokova, A. E. Hramov, V. V. Grubov, A. A. Ovchinnkov, and A. A. Koronovsky. On-off intermittency of thalamo-cortical oscillations in the electroencephalogram of rats with genetic predisposition to absence epilepsy. *Brain Res.*, 1436:147–156, 2012.

123. M. Goodfellow, K. Schindler, and G. Baier. Intermittent spike-wave dynamics in a heterogeneous, spatially extended neural mass model. *NeuroImage*, 55:920–932, 2011.
124. J. Milton and J. Foss. Oscillations and multistability in delayed feedback control. In H. G. Othmer, F. R. Adler, M. A. Lewis, and J. C. Dallon, editors, *Case Studies in Mathematical Modeling: Ecology, Physiology and Cell Biology*, pages 179–198, Upper Saddle River, NJ, 1997. Prentice Hall.
125. G.B. Ermentrout. *XPPAUT 5.91 – the differential equations tool*. Department of Mathematics, University of Pittsburgh, Pittsburgh, PA, 2005.
126. G.B. Ermentrout. *Simulating, Analyzing and Animating Dynamical Systems: A Guide to XPPAUT for Researcher and Students*. SIAM, Philadelphia, PA, 2002.
127. L.F. Shampine and S. Thompson. Solving DDEs in MATLAB. *Appl. Num. Math.*, 37:441–458, 2001.
128. K. Engelborghs, T. Luzyanina, and G. Samaey. DDE-BIFTOOL v. 2.00: a MATLAB package for bifurcation analysis of delay differential equations. Technical Report TW-330, Department of Computer Science, K.U. Leuven, Leuven, Belgium, 2001.
129. K. Engelborghs, T. Luzyanina, and D. Roose. Numerical bifurcation analysis of delay differential equations using DDE-BIFTOOL. *ACM Trans. Math. Software*, 28(1):1–21, 2002.